



# Effect of MnTiO<sub>3</sub> surface treatment on the performance of dye-sensitized solar cells

Kokn-Nara Bae<sup>a</sup>, Suk In Noh<sup>a</sup>, Hyo-Jin Ahn<sup>b,\*</sup>, Tae-Yeon Seong<sup>a,\*\*</sup>

<sup>a</sup> Department of Materials Science and Engineering, Korea University, Seoul 136-713, South Korea

<sup>b</sup> Department of Materials Science and Engineering, Seoul National University of Science and Technology, Seoul 139-743, South Korea

## ARTICLE INFO

### Article history:

Received 4 December 2012

Accepted 12 January 2013

Available online 23 January 2013

### Keywords:

Surface treatment

MnTiO<sub>3</sub>

Chemical bath deposition

Dye-sensitized solar cell

## ABSTRACT

We investigate the effect of MnTiO<sub>3</sub> surface treatment on the performance of dye-sensitized solar cells (DSSCs). The MnTiO<sub>3</sub>-treated TiO<sub>2</sub> sample reveals a smoother surface with fewer cracks than the bare TiO<sub>2</sub> sample. It is shown that the MnTiO<sub>3</sub> is an amorphous layer (~2 nm thick). The MnTiO<sub>3</sub>-treated TiO<sub>2</sub> sample exhibits higher absorbance across the wavelength region of 450–800 nm than the bare TiO<sub>2</sub> sample. The MnTiO<sub>3</sub>-treated sample gives the higher point of zero charge than the bare sample. Measurements show that the open-circuit voltage and the short circuit current are 0.64 and 0.67 V and 12.3 and 15.7 mA/cm<sup>2</sup> for DSSCs with the bare and MnTiO<sub>3</sub>-treated TiO<sub>2</sub> electrodes, respectively. The MnTiO<sub>3</sub> treatment improves the cell efficiency by about 25%.

© 2013 Elsevier B.V. All rights reserved.

## 1. Introduction

Dye-sensitized solar cells (DSSCs) work under the principle of sensitization known as Grätzel cells, which entails decoupling light absorption from charge carrier transport in a solar cell [1–3]. Conventional DSSCs consist of nanoporous semiconductors (working electrode), sensitizer (dye molecules), catalyst (counter electrode) and electrolyte of redox couple. DSSCs based on nanoporous electrodes (commonly TiO<sub>2</sub>) are of considerable interest because of their low cost, impressive efficiencies, and less toxic manufacturing process [4,5]. However, DSSCs exhibit lower conversion efficiency than silicon solar cells, because of the problems, such as charge recombination, cell leakage, long-term stability, low scalability, etc. Among them, charge recombination is a particularly serious problem, causing a significant degradation in the performance of DSSCs. For nanoporous TiO<sub>2</sub> electrode where electrons are in close proximity to holes, interfacial charge recombination serves as one of the major problems [6,7]. Thus, to suppress the recombination in the nanoporous TiO<sub>2</sub>, surface treatment processes were employed. For example, surface treatments using Al<sub>2</sub>O<sub>3</sub>, SiO<sub>2</sub>, ZrO, ZnO, and MgO were performed to minimize charge recombination [8–11]. These metal oxides on the electrode could separate the injected electrons from the oxidized electrolyte, which can slow the recombination at the TiO<sub>2</sub> surface and consequently improve the cell performance.

Manganese titanate (MnTiO<sub>3</sub>) was shown to exhibit strong absorption in the visible wavelength region, which could be beneficial to a solar energy system [12,13]. Furthermore, the conduction band edge and the surface pH of MnTiO<sub>3</sub> are higher than those of TiO<sub>2</sub> [14]. The higher conduction band edge of the MnTiO<sub>3</sub> is helpful for reducing the recombination and the basic pH at the electrode surface can attract more dye molecules. In this work, we investigate a way of improving the efficiency of DSSCs through reduction in the charge recombination and increase in the light absorption by treating the electrode surface using MnTiO<sub>3</sub>. DSSCs were also fabricated using MnTiO<sub>3</sub>-treated nanoporous TiO<sub>2</sub> electrodes (Fig. 1) and their characteristics were studied.

## 2. Experimental

A TiO<sub>2</sub> paste was prepared by combining TiO<sub>2</sub> nanoparticles (Degussa, P25) with hydroxypropyl cellulose (HPC, Aldrich), acetyl acetone, and distilled water. Nanoporous TiO<sub>2</sub> films were deposited onto transparent conducting glass substrates (F-doped SnO<sub>2</sub>, 8Ω/□, Pilkington) using TiO<sub>2</sub> paste by screen printing. The films were dried in air, followed by calcination at 500 °C for 1 h. The MnTiO<sub>3</sub> treatment was performed by dipping the samples into a mixture of 0.2 M TiCl<sub>4</sub> (Aldrich) and MnCl<sub>2</sub> (Aldrich) solutions for 30 min, followed by rinsing with DI water, and then sintering at 500 °C for 30 min in air. Finally, the films were soaked into 0.5 mM Ru(dcbpy)<sub>2</sub>(NCS)<sub>2</sub> (N719, Solaronix) in an ethanolic solution for 24 h at room temperature, and then washed with ethanol and dried in air. The counter electrode was produced by coating FTO glass substrates with a 5 mM solution of chloroplatinic acid hexahydrate

\* Corresponding author.

\*\* Corresponding author. Tel.: +82 2 3290 3288; fax: +82 2 928 3584.

E-mail addresses: [hjahn@seoultech.ac.kr](mailto:hjahn@seoultech.ac.kr) (H.-J. Ahn), [tyseong@korea.ac.kr](mailto:tyseong@korea.ac.kr) (T.-Y. Seong).

( $\text{H}_2\text{PtCl}_6 \cdot 6\text{H}_2\text{O}$ , Aldrich) in isopropanol. The coated substrates were heated at  $450^\circ\text{C}$  for 30 min. A 0.6 M BMII-based iodine solution was used as an electrolyte [15].

The structure of the samples was analyzed by X-ray diffraction (XRD, Bruker D8-Advance with  $\text{Cu K}\alpha$  radiation). The presence of the  $\text{MnTiO}_3$  was examined by X-ray fluorescence spectroscopy (XRF, Shimadzu XRF-1800). The morphologies of the samples were characterized by field-emission scanning electron microscopy (FESEM, Hitachi SU70), atomic force microscopy (AFM, SIS Nanostation II), and transmission electron microscopy (TEM, FEI Tecnai F20). Light absorption was analyzed by UV–vis spectrophotometer (Shimadzu, UV-1800). The current–voltage ( $I$ – $V$ ) characteristics of DSSCs were investigated under AM 1.5 simulate sunlight using a 150 W xenon lamp (LAB 50).

### 3. Results and discussion

Fig. 2(a) shows XRD patterns obtained from the bare- $\text{TiO}_2$  and  $\text{MnTiO}_3$ -treated  $\text{TiO}_2$  films. The characteristic diffraction peaks (indicated by the solid squares) are originated from the FTO substrate (JCPDS card No. 46-1088). The surface treatment causes no apparent shift in the diffraction peaks due to the presence of a small amount of Mn. The average grain sizes of the bare and  $\text{MnTiO}_3$ -treated  $\text{TiO}_2$  samples were calculated by the equation

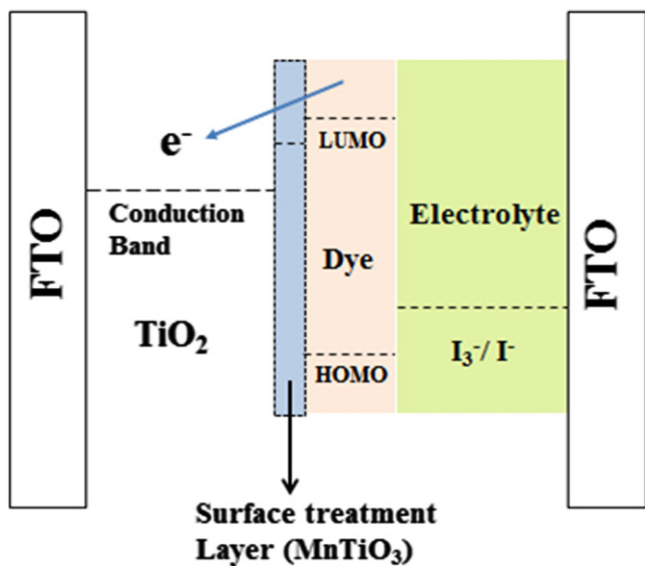


Fig. 1. Schematic diagram of a dye-sensitized solar cell.

[16],  $D = 0.9\lambda / (\beta \cos \theta)$ , where  $\lambda_{(\text{CuK}\alpha)}$  and  $\beta$  are the X-ray wavelength and the full width at half maximum (FWHM), and  $\theta$  the Bragg angle. The average sizes of the bare and  $\text{MnTiO}_3$ -treated  $\text{TiO}_2$  electrode at the main peak (101) were 26.6 and 28.2 nm, respectively. The  $\text{MnTiO}_3$  treated sample shows slightly larger size. It is noted that there are no peaks related to  $\text{MnTiO}_3$  phases. This may be due to the presence of a small amount of  $\text{MnTiO}_3$ . However, the presence of Mn was confirmed by XRF measurement, as shown in Fig. 2(b). The Mn peak is clearly seen at 63 degree.

Fig. 3(a) and (b) exhibit FESEM images of the bare and  $\text{MnTiO}_3$ -treated  $\text{TiO}_2$  samples. Comparison shows that the  $\text{MnTiO}_3$ -treated  $\text{TiO}_2$  sample reveals fewer cracks (marked 'C') than the bare  $\text{TiO}_2$  sample. Besides, comparison of the higher magnification images (Fig. 3(c) and (d)) shows that the  $\text{MnTiO}_3$ -treated  $\text{TiO}_2$  sample contains larger particles than the bare sample. The root-mean square (RMS) roughness was measured to be 86.2 and 67.4 nm for the bare and  $\text{MnTiO}_3$ -treated samples, respectively. This implies that the  $\text{MnTiO}_3$  treatment causes a smoother surface by filling the cracks (Fig. 3(a) and (b)). Fig. 3(e) and (f) reveal high resolution TEM images obtained from the bare and  $\text{MnTiO}_3$ -treated  $\text{TiO}_2$  samples. A comparison clearly shows that there is an amorphous layer ( $\sim 2$  nm thick) (as indicated by the arrows) on the treated  $\text{TiO}_2$  sample, which is believed to be a  $\text{MnTiO}_3$  layer. The  $\text{MnTiO}_3$  effectively connects the  $\text{TiO}_2$  particles, which facilitates the migration of the photo-injected electrons to the  $\text{TiO}_2$  conduction band. Consequently, the internal resistance was reduced by efficient electron migration in the  $\text{TiO}_2$  electrode [17].

Fig. 4(a) shows UV–vis absorption spectra from the dye-loaded films. The  $\text{MnTiO}_3$ -treated  $\text{TiO}_2$  sample reveals higher absorbance across the 450–800 nm wavelength region than the bare  $\text{TiO}_2$  sample. This means that the  $\text{MnTiO}_3$  treatment causes the dye molecules to more effectively attach to the  $\text{TiO}_2$  electrode. Since the N719 dye molecules terminated with carboxyl group ( $-\text{COOH}$ ) are connected to the metal oxide surface, the pH of the metal oxides is important for chemisorption between sensitizer and semiconductor. The dye molecules adhere more efficiently to the oxide electrodes if the pH of the oxide electrodes were more basic than the pH of the bare electrode [18]. The point of zero charge ( $\text{pH}_{\text{ZPC}}$ ) that is known as the surface charge is used to represent the pH of the metal oxide. The point of zero charges of the bare and the  $\text{MnTiO}_3$ -treated  $\text{TiO}_2$  samples were calculated to be 5.80 and 7.83, respectively, [14] showing that the  $\text{MnTiO}_3$ -treated sample gives higher  $\text{pH}_{\text{ZPC}}$  than the bare sample. Consequently, the  $\text{MnTiO}_3$  treatment would increase the amount of the dye molecules adhering to the electrode.

Fig. 4(b) exhibits the  $I$ – $V$  characteristics of DSSCs fabricated with and without the  $\text{MnTiO}_3$  treatment. Measurements show that the open-circuit voltage ( $V_{\text{OC}}$ ), the short circuit current ( $J_{\text{SC}}$ )

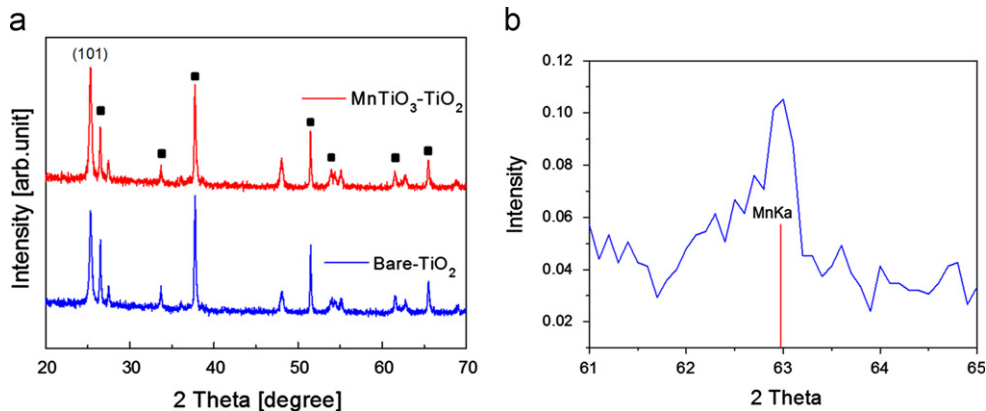
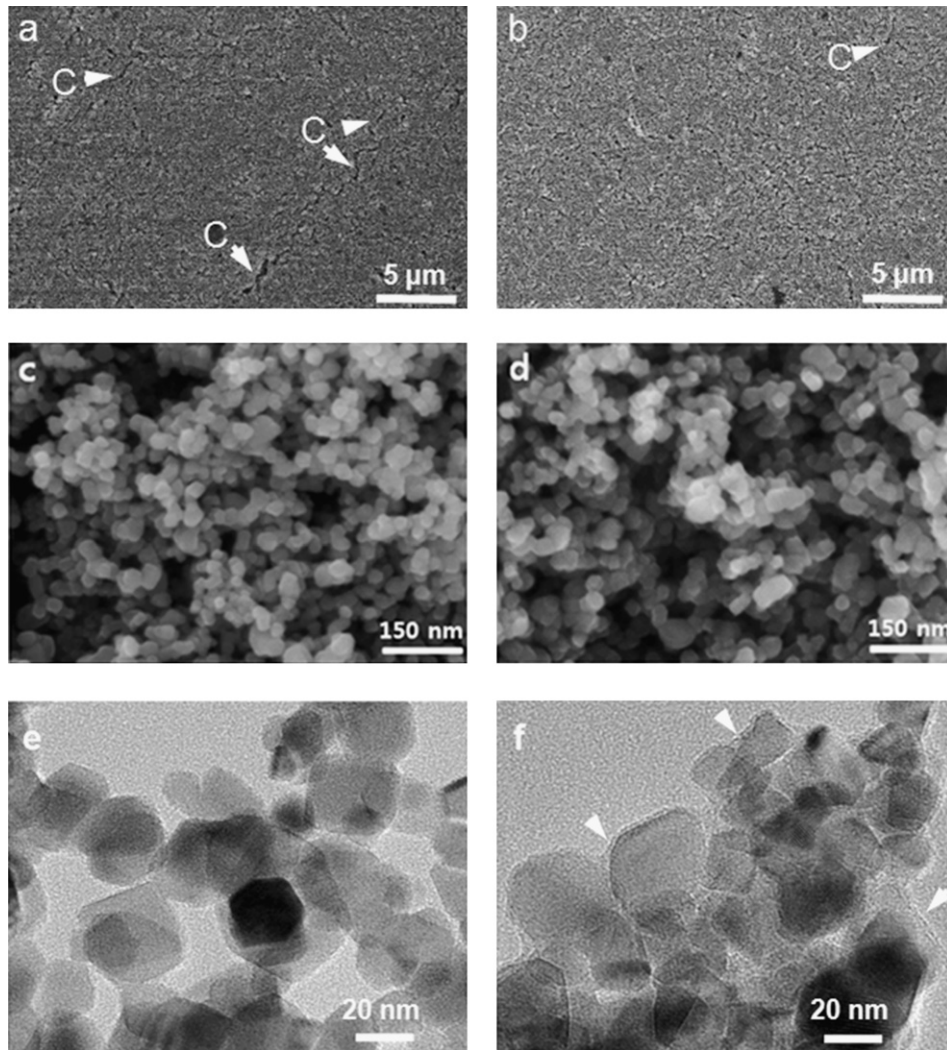
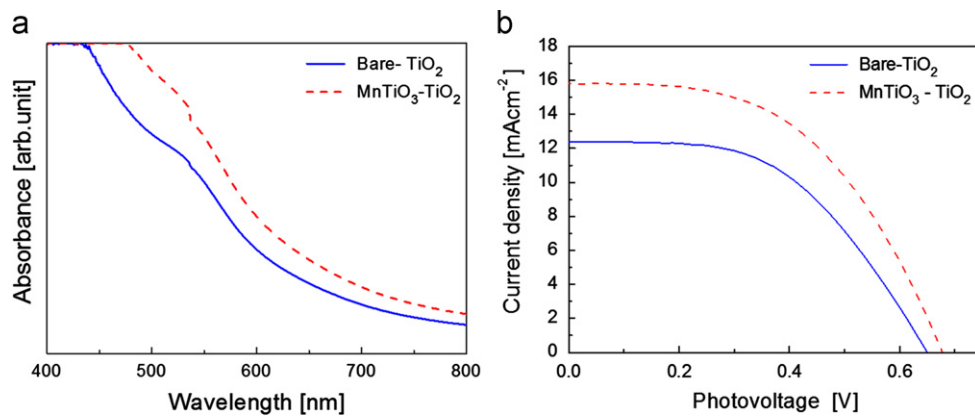


Fig. 2. (a) XRD patterns from bare and  $\text{MnTiO}_3$ -treated  $\text{TiO}_2$  films. (b) An XRF result of a  $\text{MnTiO}_3$ -treated  $\text{TiO}_2$  film.



**Fig. 3.** SEM images of (a) bare and (b) MnTiO<sub>3</sub>-treated TiO<sub>2</sub> samples. Higher magnification SEM images of (c) bare and (d) MnTiO<sub>3</sub>-treated TiO<sub>2</sub> samples. High resolution TEM images obtained from (e) bare and (f) MnTiO<sub>3</sub>-treated TiO<sub>2</sub> films.



**Fig. 4.** (a) UV-vis absorption spectra of dye-loaded samples. (b)  $I$ - $V$  characteristics of DSSCs with and without MnTiO<sub>3</sub> surface treatment.

and the fill factor are 0.64 and 0.67 V, 12.3 and 15.7 mA/cm<sup>2</sup>, and 0.51 and 0.52 for the DSSCs with the bare and MnTiO<sub>3</sub>-treated TiO<sub>2</sub> electrodes, respectively. A comparison demonstrates that after the MnTiO<sub>3</sub> treatment, the cell efficiency ( $\eta$ ) is improved by about 25% (from 4.29% to 5.37%) due to the increase in  $J_{SC}$  and  $V_{OC}$ . The enhancement in  $J_{SC}$  of the MnTiO<sub>3</sub>-treated sample can be explained as follows. First, it can be related to an increase in the

amount of the absorbed dye due to the increase in the pH of the surface-treated layer. Second, the improvement can be attributed to the decrease in the density of surface cracks (Fig. 3(b)) and the more efficient connections between the TiO<sub>2</sub> particles due to the amorphous MnTiO<sub>3</sub>. The improved  $V_{OC}$  can be explained as follows. The conduction band edge ( $E_{CB}$ ) of the MnTiO<sub>3</sub> (−4.04 eV) is higher than that of the TiO<sub>2</sub> (−4.21 eV). Thus, the

higher  $E_{CB}$  for the surface-treated layer suppresses recombination and back transfer between the  $TiO_2$  electrode and the electrolyte.

#### 4. Summary

We demonstrated a method of modifying  $TiO_2$  electrode surface regions using  $MnTiO_3$ . The  $MnTiO_3$  layer was used as a blocking layer to reduce the recombination and back transfer between the  $TiO_2$  electrode and the electrolyte. The  $MnTiO_3$ -treated sample gave the higher point of zero charge ( $pH_{ZPC}=7.83$ ) than the bare sample ( $pH_{ZPC}=5.80$ ), namely, the  $MnTiO_3$ -treated sample was more basic than the bare sample. DSSCs with the  $MnTiO_3$ -treated sample showed higher open-circuit voltage of 0.67 V and higher short circuit current of 15.7 mA/cm<sup>2</sup>, leading to about 25% higher cell efficiency compared to DSSCs with the bare electrodes. This indicates that the  $MnTiO_3$  treatment could represent a promising processing tool for the fabrication of high-performance DSSCs.

#### Acknowledgment

This work was supported by the World Class University program through the National Research Foundation of Korea funded by MEST (R33-2008-000-10025-0).

#### References

- [1] O'Regan B, Grätzel M. Nature 1991;353:737–40.
- [2] Hod I, Shalom M, Tachan Z, Rühle S, Zaban A. J Phys Chem C 2010;114:10015–8.
- [3] Wu J, Lan Z, Hao S, Li P, Lin J, Huang M, et al. Pure Appl Chem 2008;80:2241–58.
- [4] Grätzel M. J Photochem Photobiol C 2003;4:145–53.
- [5] Nazeeruddin K, Baranoff E, Grätzel M. Sol Energy 2011;85:1172–8.
- [6] Hagfeldt A, Grätzel M. Chem Rev 1995;95:49–68.
- [7] Yum JH, Nakade S, Kim DY, Yanagida S. J Phys Chem 2006;110:3215–9.
- [8] Menzies D, Dai Q, Cheng Y-B, Simon GP, Spiccia L. Mater Lett 2005;59:1893–6.
- [9] Palomares E, Clifford JN, Haque SA, Lutz T, Durrant JR. J Am Chem Soc 2003;125:475–82.
- [10] Wang ZS, Huang CH, Huang YY, Hou Y, Xie PH, Zhang BW, et al. Chem Mater 2001;13:678–82.
- [11] Wu S, Han H, Tai Q, Zhang J, Xu S, Zhou C, et al. Nanotechnology 2008;19:215704–21579.
- [12] Zhou G, Kang Y. Mater Sci Eng C 2004;24:71–4.
- [13] Song ZQ, Wang SB, Yang W, Li M, Wang H, Yan H. Mater Sci Eng B 2004;113:121–4.
- [14] Xu Y, Schoonen MAA. Am Mineral 2000;85:543–56.
- [15] Ito S, Chen P, Comte P, Nazeeruddin M, Liska P, Péchy P, et al. Prog Photovolt: Res Appl 2007;15:603–12.
- [16] Cullity BD. Elements of X-ray diffraction. 2nd ed. Massachusetts: Addison-Wesley Reading; 1978.
- [17] Menzies D, Dai Q, Bourgeois L, Caruso R, Cheng YB, Simon G, et al. Nanotechnology 2007;18:125608–18.
- [18] Jung H, Lee JK, Nastasi M, Lee SW, Kim JY, Park JS, et al. Langmuir 2005;21:10332–5.